Taxane-Induced Blockade to Nuclear Accumulation of the Androgen Receptor Predicts Clinical Responses in Metastatic Prostate Cancer

Medha S. Darshan[1,#], **Matthew S. Loftus**[1,#], **Maria Thadani-Mulero**[1], **Ben P. Levy**[1], **Daniel Escuin**[2], **Xi Kathy Zhou**[4,5], **Ada Gjyrezi**[1], **Chantal Chanel-Vos**[1], **Ruoqian Shen**[1,3], **Scott T. Tagawa**[1,3,5], **Neil H. Bander**[3,5], **David M. Nanus**[1,3,5], and **Paraskevi Giannakakou**[1,5,*]

[1]Department of Medicine, Division of Hematology and Medical Oncology, Weill Cornell Medical College of Cornell University, New York, NY 10021

[2]Medical Oncology Department, Institut de Recerca, Hospital de la Santa Creu i Sant Pau, Barcelona, Spain

[3]Department of Urology, Weill Cornell Medical College of Cornell University, New York, NY 10021

[4]Department of Public Health, Division of Biostatistics and Epidemiology, Weill Cornell Medical College of Cornell University, New York, NY 10021

[5]Weill Cornell Cancer Center, New York, NY 10021

Abstract

Prostate cancer progression requires active androgen receptor (AR) signaling which occurs following translocation of AR from the cytoplasm to the nucleus. Chemotherapy with taxanes improves survival in patients with castrate resistant prostate cancer (CRPC). Taxanes induce microtubule stabilization, mitotic arrest and apoptotic cell death, but recent data suggest taxanes can also affect AR signaling. Here we report that taxanes inhibit ligand-induced AR nuclear translocation and downstream transcriptional activation of AR target genes such as PSA. AR nuclear translocation was not inhibited in cells with acquired β-tubulin mutations that prevent taxane-induced microtubule stabilization, confirming a role for microtubules in AR trafficking. Upon ligand activation, AR associated with the minus-end microtubule motor dynein, thereby trafficking on microtubules to translocate to the nucleus. Analysis of circulating tumor cells (CTCs) isolated from the peripheral blood of CRPC patients receiving taxane chemotherapy revealed a significant correlation between AR cytoplasmic sequestration and clinical response to therapy. These results indicate that taxanes act in CRPC patients at least in part by inhibiting AR nuclear transport and signaling. Further they suggest that monitoring AR subcellular localization in the CTCs of CRPC patients might predict clinical responses to taxane chemotherapy.

INTRODUCTION

Prostate cancer (PC) is the most commonly diagnosed cancer and the second leading cause of cancer-related death in men in the United States. In PC, growth and disease progression requires active androgen receptor (AR) signaling, which occurs following translocation of AR from the cytoplasm to the nucleus where AR, acting as a transcription factor, binds to and activates AR-target genes [1–3]. Continued AR signaling remains essential to PC progression following androgen withdrawal (castration), with recent data suggesting that

---

*To whom correspondence should be addressed: pag2015@med.cornell.edu.
#The first two authors contributed equally to the work

intra-tumoral androgen synthesis stimulates PC growth in patients with castrate resistant prostate cancer (CRPC) [4]. Agents that target the AR signaling axis in patients with CRPC have recently demonstrated significant clinical activity in patients with CRPC [5], corroborating the importance of AR as a therapeutic target in CRPC patients.

Cytotoxic chemotherapy has been used to treat patients with advanced PC for over 20 years [6]. However, the taxanes represent the only class of chemotherapy agents demonstrated to improve survival of patients with metastatic CRPC; docetaxel and recently cabazitaxel are the standard for CRPC treatment [7–9]. At the cellular level, taxanes bind β-tubulin and stabilize the microtubule cytoskeleton which, in actively dividing cells leads to mitotic arrest and apoptotic cell death [10]. However, in contrast to cancer cells cultured *in vitro*, cancer cells in patients often display very slow doubling times [11, 12], suggesting that the clinical activity of taxanes cannot be attributed solely to their antimitotic effects and that it is important to understand the functional consequences of taxane-induced microtubule stabilization in cells during interphase [13]. Accordingly, we have previously shown that dynamic interphase microtubules regulate the intracellular transport and activity of two other transcription factors, p53 and HIF-1α [14–17]. A number of recent reports by us and others suggest that taxane chemotherapy can inhibit AR signaling in PC cells [18–20]. Here, we define the mechanisms of taxane inhibition of AR and propose AR localization in PC circulating tumor cells (CTCs) as a predictor of response/resistance to taxane chemotherapy in patients with CRPC.

MATERIALS AND METHODS

Cell culture and antibodies

The prostate cancer cell lines LNCaP, PC3 and PC3/AR were derived and maintained as previously described [21–23]. The PC3/mCherry-tubulin cell line was generated in our laboratory by stably transfecting PC3 prostate cancer cells with pcDNA3:mCherry-tubulin plasmid which was a generous gift from the laboratory of Dr. Tsien (UCSD, CA) and selecting transfected cells with 200 µg/ml neomycin (G418). The following antibodies were used for immunofluorescence staining and western blotting: rabbit polyclonal anti-AR (N-20) and goat polyclonal anti-PSA (C-19) from Santa Cruz Biotechnology, Inc (Santa Cruz, CA), mouse monoclonal anti-prostate-specific membrane antigen (PSMA) J591 [24, 25], rat monoclonal anti α-tubulin was from Novus Biologicals (Littleton, CO), mouse monoclonal anti-c-myc was from Oncogene Research Products (Darmstadt, Germany), mouse monoclonal antibody against dynein intermediate chain (IC74) was from Covance (Emeryville, CA). All the Alexa conjugated secondary antibodies were from Molecular probes (Eugene, OR). NLP-005 Methyltrienolone (R1881) was purchased from Perkin Elmer (Boston, MA). Paclitaxel and docetaxel were from Sigma.

Determination of secreted PSA levels

LNCaP cells were cultured on 6 well plates and treated overnight with either docetaxel at the indicated concentrations or the di-hydroxytestosterone (DHT) analog, R1881, at 10 nM for 1 hr or the combination of R1881 treatment following incubation with docetaxel. Supernatant were diluted 1:10 with Abbott Laboratories Free and Total PSA Specimen Diluent. Secreted PSA level measurements were made on Abbott Diagnostics IMx MEIA system (Abbott Park, IL) as previously described [18].

Measurement of PSA-luciferase activity

LNCaP cells were transiently co-transfected with a dual-luciferase reporter assay system in which luciferase is under the control of a promoter containing androgen-responsive elements (ARE-Luciferase) from the prostate-specific antigen (PSA) gene (Promega Corp., Madison,

WI) [26] and pRL-TK-luc, *Renilla* luciferase reporter construct (kindly provided by P. Vertino, Emory University, Atlanta, GA), upon reaching 60% confluency on 6 well plates. Thirty hours post-transfection cells were incubated overnight with either DMSO (vehicle control) or taxanes (paclitaxel or docetaxel) at the indicated concentrations followed by 1 hr treatment with R1881 at either 1nM or 10nM concentration. Cells were harvested and cell lysates were prepared for luciferase assays. Each transfection experiment was performed in triplicate. Results represent an average of at least three independent biological repeats with data presented as relative PSA luciferase activity normalized to *Renilla* luciferase values.

Establishment of 1A9 cancer cell lines overexpressing AR

The parental ovarian cancer cells 1A9 and their derived beta-tubulin mutant, paclitaxel-insensitive clone PTX10 [27] were transfected with a pFLAG-hAR plasmid using lipofectamine (Invitrogen) following the manufacturer's instructions. Cells were selected using G418 (300 ug/ml) and AR-expressing clones (as verified by Western Blot analysis) were named 1A9/AR and PTX10/AR cells, respectively. To evaluate AR trafficking to the nucleus, 1A9/AR and PTX10/AR cells were plated on Cell-tak-coated coverslips in RPMI 1640 containing 10% FCS and switched to medium containing 10% charcoal stripped serum (CS) for 72 hours. Following treatments without (control) or with 1) DHT (100 nM) for 2 hours; or 2) PTX (100 nM) for 2 hrs, followed by DHT (100 nM) for 2 hours, cells were fixed with PHEMO buffer [16] and immunostained using antibodies against AR (PG21, Millipore, 1:200) and alpha tubulin (1:1000) followed by Alexa 647 (1:1000) and Alexa 568 (1:500) secondary antibodies and DAPI staining.

Western blotting and immunoprecipitation

Control untreated and treated cells were lysed in TNES buffer containing 50 mM Tris (pH 7.5) 100 mM NaCl, 2 mM EDTA, 1% Nonidet P-40, and a 1X protease inhibitor mixture (Roche Applied Science). For the immunoprecipitation experiments, 0.5 mg of soluble cell extract was immunoprecipitated with either a rat α-tubulin or a mouse antibody directed against dynein intermediate chain (IC74) and their respective IgG controls, using protein-G plus agarose (Calbiochem, Darmstadt, Germany) as recommended by the manufacturer. Immunoprecipitated proteins and 50 μg of total cell extracts were resolved by 10% SDS-PAGE and immunoblotted for the indicated proteins. Immunoblots were analyzed with the Odyssey infrared imaging system (LI-COR, Lincoln, NE).

Dynamitin overexpression

For the dynamitin overexpression experiments, LNCaP and PC3-AR cells were plated on 12mm glass coverslips (Electron Microscopy Sciences, Hatfield, PA) and transiently transfected with c-myc-tagged pCMVH50m plasmid containing dynamitin, a kind gift from R. Vallee (Columbia University, New York, NY) [28]. All transfections were performed using FuGENE 6 transfection reagent (Roche Applied Science, Indiananpolis, IN) according to the manufacturer's recommendations. C-myc-dynamitin transfected cells were processed for immunofluorescence labeling using the following primary antibodies: anti-AR rabbit polyclonal and an anti-c-Myc mouse monoclonal. The secondary antibodies used were Alexa 488-conjugated goat anti-rabbit immunoglobulin G (IgG; 1:500) and Alexa 568-conjugated goat anti-mouse IgG (1:500). Cells were then analyzed by confocal microscopy.

Microtubule co-sedimentation assay

LNCaP cells were lysed in low salt buffer (LSB) (20 mM Tris, 1 mM MgCl$_2$, 2 mM EGTA, 0.5% NP-40 and 1X cocktail protease inhibitors). 20 μl of MAP-rich bovine brain tubulin (5 mg/ml) (Cytoskeleton, Denver, CO) was supplemented with 1 mM GTP and 2.5 μl cushion buffer consisting of PEM buffer (80 mM PIPES, 1 mM MgCl$_2$, 1 mM EGTA) in 50%

glycerol and allow to polymerized at 35°C for 20 min. Microtubules were diluted in 200μl warm PEM plus 20 μM paclitaxel (PTX) and kept at room temperature. Alternatively, MAP-rich tubulin was kept on ice and supplemented with PEM buffer plus 20 μM colchicine to prevent microtubule polymerization. 20 μl of either microtubules or tubulin dimers were incubated with 50 μg of LNCaP total cell extracts for 30 min at 35°C or 4°C respectively. Samples were loaded into 100 μl cushion buffer and microtubules were pelleted by centrifugation at 100,000g at room temperature in an airfuge (Beckman Coulter, Inc., Fullerton, CA). The warm supernatant (WS) or cold supernatant (CS) were separated and the warm (WP) or cold pellet (CP) were resuspended in an equal volume of PEM buffer. 35 μl from each fraction were loaded in a 10% SDS-PAGE and western blotting was performed with antibodies against AR (1:200 dilution) and α-tubulin (clone YL1/2, 1:5000 dilution).

Live cell recording of AR nuclear translocation

For the analysis of GFP-AR trafficking in PC3-mCherry-tubulin cells, PC3-mcherry-tubulin cells were plated on 35mm MatTek dishes and microinjected with full-length GFP-AR. The cells were grown in complete RPMI media and switched to phenol-red free media supplemented with 5% charcoal-stripped medium for up to 3 hours before imaging. Cells were transferred to a live-cell chamber and maintained at 37°C and 5% CO2 using the Tokai Hit Temperature control unit INUG2-ZILCS. The AR ligand R1881 was added to the cells using a Tokait Hit perfusion pipe/tube set with Luer lock syringe. Live cell imaging was performed by acquiring 0.5 μm Z-sections through the entire cell depth at each time point using a Zeiss confocal microscope fitted with a Spinning Disk unit manufactured by Yokogawa Electric Corporation and run with the Axiovision software. Images were acquired using the 488 laser to monitor GFP-AR subcellular localization. Simultaneous imaging of both the GFP-AR and mCherry-tubulin fluorophores was not possible due to the low photostability of the mCherry fluorophore. Therefore, mCherry-tubulin was imaged once at the end of each recording to reveal the pattern of the microtubule cytoskeleton. Representative fields were selected and images (z-stacks) were acquired at 10 min intervals for a total of 2 hr. Maximum intensity projections were made with the Axiovision software, AxioVision files were saved as 16-bit images and exported to MetaMorph image analysis software. Background subtraction was performed using the mean pixel value of a noncell region on each image with the statistical correction function in MetaMorph and a sum projection was assembled from the images recorded at 10 min intervals. High-intensity pixels in noncellular regions or regions not of interest were also scaled out. Nuclear versus cytoplasmic AR values were obtained using integrated pixel intensity values from the sum projection and the percentage of nuclear AR was calculated using the following formula: % Nuclear AR = 100*Nuclear AR/Total AR.

Venous blood collection and isolation of circulating tumor cells (CTCs)

Following approval of the Weill Cornell Institutional Review Board (IRB), 10 mls of peripheral blood was collected, in sodium citrate tubes (BD, Franklin Lakes, NJ), from CRPC patients at various timepoints during taxane chemotherapy. CTCs were then isolated using the epithelial cell adhesion molecule (EpCAM)-based immunomagnetic capture CellSearch system as per the manufacturer's instructions [29]. This enrichment step greatly facilitated our analysis as CTCs are very rare (1 in 10^6 PBMCs) and require specialized technology for their detection. CellSearch has been the first and only FDA-approved CTC detection technology utilized for clinical prognosis. Following the isolation/enrichment step with the CellTracks AutoPrep System®, captured CTCs were cytospun onto Cell-Tak-(BD Biosciences, San Jose, CA) -coated coverslips and processed for immunofluorescence staining. For our analysis, we performed only the first step of enrichment and omitted the second step of automated staining with cytokeratins, DAPI and CD45 which is used for CTC

enumeration. In addition, to ensure analysis of PC CTCs among the leucocytes present in the EpCAM-enriched cell population, we stained for PSMA (prostate specific marker) and CD45 (leucocyte specific marker) and analyzed the PSMA+/CD45- cells for AR subcellular localization using multiplex confocal microscopy. Using this methodology we monitored longitudinally CRPC patients receiving taxane-chemotherapy and investigated the association between AR subcellular localization in CTCs and patients' clinical response to therapy.

In parallel, CTCs were also identified following Ficoll separation of blood collected in Vacutainer Cell Preparation Tube with Sodium Heparin (BD, Franklin Lakes, NJ). The PBMC layer containing CTCs was collected and washed in 1X PBS. Hemolysis was performed using ammonium chloride buffer (150 mM NH_4Cl, 10 mM $NaHCO_3$, 1 mM Na_2EDTA, pH adjusted to 7.3). Cells were counted by Bright-Line hemacytometer (Hausser Scientific, Horshan, PA) and approximately 1×10^6 cells were plated on cell-tak coated 8-mm glass coverslips (Electron Microscopy Sciences, Hatfield, PA) in 48 well plates, cytospun and allowed to attach. Subsequent to attachment, cells were fixed and processed for immunofluorescence and confocal microscopy as described below.

Immunofluorescence and confocal microscopy

Following treatment and attachment, the cells, including PBMCs were fixed and processed for immunofluorescence labeling [16]. The following antibodies were used: rabbit polyclonal antiAR, mouse monoclonal anti-PSMA (J591) and rat monoclonal anti α-tubulin. The secondary antibodies used were Alexa 488-conjugated goat anti-rabbit immunoglobulin G (IgG; 1:500), Alexa 568-conjugated goat anti-mouse IgG (1:500) and Alexa 647-conjugated goat anti-rat IgG (1:500). DNA was stained with 13g ml^{-1} 4, 6-diamidino-2-phenylindole, DAPI (Sigma, St. Louis, MO). The cells were mounted using Mowiol (Calbiochem, Darmstadt, Germany) and imaged using a Zeiss LSM 5 LIVE (Thornwood, NY) confocal microscope using 63x/1.4 Plan APOCHROMAT and 100x/1.4 Plan APOCHROMAT objectives. All images were acquired and analyzed using Zeiss LSM 5 LIVE software.

Quantitation of AR subcellular localization in CTCs

CTCs were obtained by CellSearch enrichment or Ficoll separation for each patient at each time point. CTCs were imaged with a Zeiss 5 LIVE confocal microscope using a 20X objective. A single plane image of each cell was taken and analyzed using the MetaMorph imaging software (Molecular Devices). The nuclear region of the CTC was identified by DAPI staining. Total cellular AR fluorescence intensity was measured and the amount of AR fluorescence inside the nuclear region was determined, allowing us to calculate the percentage of AR in the cytoplasm and the nucleus of each CTC. The total number of CTCs analyzed varied among patients, ranging from 3 to 27 CTCs per patient per time point. When possible we analyzed at least 10 CTCs per patient per time point.

Statistical Analysis

For CTCs isolated from the fourteen patients, we determined both the AR subcellular localization and total AR fluorescence intensity at each patient visit. AR localization was defined as follows: if greater than 50% of CTCs in a given sample have a meaningful percentage of AR in cytoplasm (>40%), we considered AR localization as cytoplasmic, otherwise, we considered AR localization as nuclear. Patients' data with clear PSA outcomes (progressing or response/stable disease) was included in the analysis. Fisher's exact test was used to correlate AR localization in the nucleus with the patients' clinical response to treatment assessed using PSA working group 2 criteria. Considering the longitudinal nature of the data, the association between the AR measurements and the PSA

outcome was more rigorously assessed using the generalized linear mixed effects models [30–32]. Effects with p-values <0.05 was considered statistically significant.

RESULTS

Taxanes inhibit AR nuclear accumulation and signaling

Since microtubules are involved in transcription factor trafficking, we investigated the effects of taxane treatment on AR nuclear translocation in LNCaP PC cells. Cells were treated with paclitaxel (PTX) followed by the addition of the di-hydrotestosterone (DHT) analog R1881 (Fig. 1A–C) and analyzed for evidence of PTX-induced microtubule bundling and R1881-induced AR nuclear accumulation by confocal microscopy. Interestingly, PTX induced a significant decrease in AR nuclear accumulation, at both baseline and following R1881 treatment (Fig. 1A–C). Quantitation of the extent of PTX-induced AR nuclear exclusion revealed a significant decrease in the percentage of cells with nuclear AR, following R1881 treatment, from 70% to <30% (Fig. 1B; p<0.001) and a concomitant 50% decrease in the total fluorescence intensity of nuclear AR staining (Fig. 1C; p<0.001). The profound cytoplasmic sequestration of AR following paclitaxel treatment implicated microtubules in the shuttling of the receptor from the cytoplasm to the nucleus. To explore the dynamics of ligand induced AR nuclear translocation, we introduced full-length GFP-AR into PC3 cells stably expressing mCherry tubulin (PC3:mCherry-tub) (Fig. 1D and time lapse confocal microscopy recordings available as movies S1 and S2). Paclitaxel treatment significantly reduced the extent and the rate of AR nuclear accumulation in cells with stabilized microtubules as early as 30 min post R1881 addition (p<0.01-0.001). Consistent with drug-induced AR nuclear exclusion, we also observed dose-dependent inhibition of AR transcriptional activity using a luciferase reporter assay in LNCaP cells expressing endogenous AR (Fig. 2A). Similarly, docetaxel (DTX) treatment inhibited ligand-induced protein expression (Fig. 2B) and secretion of prostate specific antigen (PSA; Fig. 2C), an AR target gene used clinically to monitor biochemical disease progression in men with PC [18, 33]. Together, these results suggested that taxanes inhibit AR signaling by preventing AR nuclear accumulation.

Microtubule stabilization is a prerequisite for taxane-induced inhibition of AR signaling

To determine whether the taxane-induced cytoplasmic sequestration of AR required prior microtubule stabilization, we utilized an isogenic model of paclitaxel- sensitive and - resistant human ovarian cancer cells, 1A9 and 1A9/PTX10, respectively, stably transfected with wild-type GFP-AR. Drug resistance in 1A9/PTX10 cells is conferred by an acquired tubulin mutation (Fβ270V) at paclitaxel's binding site [27]. Paclitaxel treatment of taxane-resistant 1A9/PTX10 cells had no effect on GFP-AR subcellular localization (Fig. 3, right panel) (consistent with the drug's inability to stabilize microtubules), whereas DHT-induced GFP-AR nuclear accumulation was robustly inhibited by paclitaxel in parental drug-sensitive 1A9 cells (Fig. 3, left panel). These results demonstrated that the microtubule stabilizing activity of taxanes is required to inhibit AR translocation and downstream signaling; further implying that in cases where the drug-target interaction is impaired AR signaling will remain unaffected. To further characterize the interaction of AR with microtubules, we performed high resolution multiplex confocal microscopy in PC3 cells stably expressing AR, and observed a clear co-localization of cytoplasmic AR with intact microtubules. Following taxane treatment AR remained associated with bundled microtubules in the perinuclear region (Fig. 4A). The tubulin-AR association was confirmed by coimmunoprecipitation of tubulin and AR in LNCaP cells (Fig. 4B) as well as by a microtubule cosedimentation assay [14] in which AR was found preferentially associated with the microtubule polymer fraction (WP) and not the fraction containing soluble tubulin

dimers (WS), lending further support to the role of microtubules as tracks for AR transport towards the nucleus (Fig. 4C).

The microtubule-associated motor protein, dynein, mediates AR trafficking

To test this hypothesis, we investigated the involvement of the minus-end-directed microtubule-motor protein dynein, which transports cargo from the cytoplasm towards the nucleus, in AR trafficking [34]. Coimmunoprecipitation experiments revealed that AR associated with dynein, and that this interaction was increased upon ligand (R1881) induced AR nuclear translocation (Fig. 5A). In addition, dynein co-fractionated with AR and microtubules in the co-sedimentation assay (Fig. S1A), suggesting that both dynein and AR associate preferentially with microtubule polymers. Cytoplasmic dynein, in order to drive subcellular motile functions, works in concert with several accessory proteins including dynactin, an adapter that mediates the binding of dynein to cargo structures enhancing the motor's processivity. Overexpression of the dynactin associated protein dynamitin, which disrupts the dynein-cargo interaction [28], markedly reduced AR nuclear accumulation following R1881 induction (Fig. 5B and Fig. S1B), suggesting that following ligand binding, AR is shuttled from the cytoplasm to the nucleus via microtubules and its associated motor complexes.

AR cytoplasmic localization in CTCs correlates with clinical response to taxane chemotherapy

To assess whether taxanes inhibit AR nuclear translocation *in vivo*, we isolated CTCs from the blood of CRPC patients and examined PSMA (prostate specific membrane antigen) [24, 25, 35, 36] expressing CTCs by high resolution confocal microscopy. We first confirmed colocalization of AR with the microtubule cytoskeleton in patient samples (Fig. 6A). We next investigated whether perturbation of the microtubule-AR axis in CTCs identified in CRPC patients receiving taxane chemotherapy would correlate with clinical response. As shown in Figure 6B (top panel), CTCs from a patient who was refractory to paclitaxel chemotherapy exhibited an unperturbed microtubule network with AR present in both the nucleus and cytoplasm. In contrast, in a second patient who was responding to docetaxel chemotherapy, CTCs demonstrated bundled microtubules and AR was exclusively in the cytoplasm with intense AR perinuclear staining (Fig. 6B, lower panel). These results in 2 patients suggested that taxane-induced microtubule bundling and AR cytoplasmic localization correlated with clinical response to chemotherapy. We therefore expanded our analysis to additional patients and used CTCs enriched from the blood of CRPC patients using EpCAM-based immunomagnetic capture (CellSearch) [29]. To identify PC CTCs among the leucocytes present in the EpCAM-enriched cell population, we stained for PSMA and CD45 (leucocyte specific marker) and analyzed the PSMA+/CD45− cells for AR subcellular localization using multiplex confocal microscopy (Fig. 6C). Using this methodology, we monitored longitudinally CRPC patients receiving taxane-chemotherapy and investigated the association between AR's subcellular localization in CTCs and patients' clinical response to therapy. Figure 6D shows a representative example of CTCs isolated from a metastatic CRPC patient in which AR was localized in the nucleus at baseline, consistent with this patient's rising serum PSA (Fig. 6E, open symbols), but was consistently shifted to the cytoplasm during PSA decline following chemotherapy (Figs. 6D, 6E). In another patient (Fig. 6E, filled symbols), AR was detected in the cytoplasm as early as 1 hour following paclitaxel administration which was followed by a significant decline in PSA. This result emphasizes fast and effective drug-target engagement in this patient's sample.

Table 1 summarizes the results from our CTC analyses performed on sequential blood samples obtained from fourteen patients receiving taxane chemotherapy and followed

longitudinally. PSA outcomes were assigned by clinicians independent of CTC enumeration using modified Prostate Cancer Working Group 2 criteria [33]. Responders were defined as having at least a 30% reduction in PSA [33, 37, 38]; progressors had >25% increase in PSA with a minimum absolute increase of 2 ng/mL and those meeting neither criteria were considered stable. Among 18 samples obtained during clinical progression, 13 (72%) demonstrated nuclear AR localization; while among 17 responding/stable samples, 12 (70.6%) showed cytoplasmic AR localization (p-value=0.02) (Table 1). We also examined the association between longitudinal quantitative AR measurements (either in terms of the percentage of AR in cytoplasm or the total AR intensity) and the PSA outcome using a generalized linear mixed-effects model that accounts for possible clustering of data among cells from the same sample and among samples from the same subject. This analysis revealed that the odds of responding for those with AR completely in cytoplasm was estimated to be increased by 30% compared to patients with no AR in the cytoplasm (OR=exp(0.26) =1.30, P<0.001). Similarly, using log transformed total AR intensity as the predictor, we found that increased total AR intensity is associated with decreased odds of responding. With each unit increase in the log AR intensity, the odds of responding is 24% lower (OR=exp(−0.28)=0.76, P<0.001). Interestingly, we observed AR nuclear localization in all four baseline patient samples indicative of active AR signaling. In contrast, AR cytoplasmic localization was detected as early as 1 hr following the first dose of paclitaxel administration (patient 4) showcasing rapid and effective perturbation of the microtubule-AR axis. Altogether, these results demonstrate that AR subcellular localization can be resolved in CTCs and can serve as a biomarker to monitor clinical response to chemotherapy.

DISCUSSION

Prostate cancer remains a major cause of cancer related morbidity in the United States with the majority of PC related deaths resulting from metastatic, castrate resistant disease. Widely thought to be chemotherapy resistant [6], androgen withdrawal was considered the only effective therapy for patients who developed metastases. Although numerous clinical studies using taxane-based regimens had demonstrated anti-tumor activity and clinical benefit in patients with CRPC, it was only in 2004 that the taxane docetaxel was proven to significantly improve overall survival [8, 9]. In 2010, the taxane cabazitaxel was shown to improve overall survival in CRPC patients who had received prior docetaxel chemotherapy [7]. These studies have proven the clinical utility of taxanes in PC.

Historically, the antitumor activity of taxanes has been attributed to inhibition of mitosis, as mitotic cell division requires the presence of highly dynamic microtubules and taxane treatment by suppressing microtubule dynamics leads to mitotic arrest in actively dividing cancer cells growing on two-dimensional tissue culture [10]. In addition to mitosis, microtubule dynamics are critically important for many interphase cellular functions such as intracellular transport and signaling, the disruption of which by taxanes has not been functionally implicated in their antitumor activity [39]. Here we provide evidence that taxanes clinical activity in PC can be attributed at least in part to the inhibition of AR activity via its effect on microtubules. Inhibition of AR signaling as effective therapy in the castrate state has similarly been observed with agents designed to specifically target the AR axis, including the androgen synthesis inhibitor abiraterone and the novel AR antagonist MDV3100 [5]. The observation that docetaxel may also act by inhibiting AR through microtubule stabilization may explain why taxanes are the only class of active chemotherapy in CRPC, and conversely why other chemotherapeutic agents have been largely ineffective.

Previous reports have shown that taxanes can inhibit PSA expression [18–20]. Gan *et al* reported that paclitaxel inhibition of AR transactivated genes is mediated by FOXO1 [19],

whereas Zhu *et al* similarly suggested that taxanes effect on microtubules inhibits AR nuclear localization [20]. These results together with the data presented here strongly suggest that interphase microtubule functions coupled with the trafficking and signaling pathways they regulate are indeed the effective targets of taxane treatment. In the current study, we show that in cells with tubulin mutation at the paclitaxel binding site treatment with PTX does not prevent AR nuclear localization suggesting that tubulin mutations at the taxane binding site may account for clinical taxane resistance. This mechanism could also explain the lack of clinical cross-resistance between the different taxanes as we have previously reported that cancer cell lines that are resistant to paclitaxel due to acquired beta-tubulin mutations at the taxane-binding site retain sensitivity to docetaxel or other microtubule-stabilizing drugs that bind tubulin at the same site, such as the epothilones [27, 40, 41]. This is attributed to the distinct binding modes of paclitaxel, docetaxel or the epothilones in the same binding site in β-tubulin so that single point mutations may affect one taxane but not the other even though the binding site is shared [42]. Alternatively, AR gene alterations rendering AR trafficking independent of microtubule control could also lead to taxane resistance.

The lack of readily biopsied tumor material from metastatic CRPC patients represents an additional challenge to the understanding of clinical drug resistance. Circulating tumor cells isolated from the blood of metastatic cancer patients provide a non-invasive source of tumor material that can enable molecular characterization of disease progression. Previous studies have identified PC specific molecular alterations in CTCs such as AR gene amplification, PTEN loss and TMPRSS2:ERG fusion confirming the malignant origin of CTCs [43–45]. However, no studies have directly monitored CTCs for drug-induced dynamic changes in molecular pathways in individual patients over time. Using isolated CTCs from CRPC patients followed longitudinally over the course of taxane chemotherapy, we found a significant correlation between AR cytoplasmic localization and clinical response, suggesting that the changes in AR subcellular localization can be used as a predictive biomarker of response. We also detected a decrease in AR intensity. The correlation between the decrease in total AR intensity and clinical response to taxanes is consistent with AR transcriptional autoregulation [46] and our results showing that taxane treatment leads to AR cytoplasmic sequestration and subsequent inhibition of transcriptional activity (Fig 1). These results showing that disruption of the microtubule-AR axis contributes to taxane anti-tumor activity also suggest that combining a taxane with other therapies targeting AR signaling at the level of ligand synthesis [47] or ligand-receptor interaction or DNA transactivation [48] may be synergistic.

Whether studying the effect of a taxane on AR localization in CTCs can be used as predictor of clinical response to therapy requires further study. To this end, we have begun a prospective clinical trial of CRPC patients receiving docetaxel chemotherapy to determine if AR localization following chemotherapy correlates with response, and whether tubulin and/or AR mutations correlate with docetaxel resistance. The ability to monitor these events in CTCs over the course of a patient's treatment will enable early therapeutic interventions and help elucidate the mechanisms of drug-resistance in CRPC patients.

Supplementary Material

Refer to Web version on PubMed Central for supplementary material.

Acknowledgments

References

1. Feldman BJ, Feldman D. The development of androgen-independent prostate cancer. Nat Rev Cancer. 2001; 1(1):34–45. [PubMed: 11900250]

2. Petrylak DP. New paradigms for advanced prostate cancer. Rev Urol. 2007; 9(Suppl 2):S3–S12. [PubMed: 17554403]

3. Gelmann EP. Molecular biology of the androgen receptor. J Clin Oncol. 2002; 20(13):3001–15. [PubMed: 12089231]

4. Chen CD, et al. Molecular determinants of resistance to antiandrogen therapy. Nat Med. 2004; 10(1):33–9. [PubMed: 14702632]

5. Attard G, Richards J, de Bono JS. Targeting the androgen receptor signaling pathway in metastatic prostate cancer. Clin Cancer Res. 2011

6. Yagoda A, Petrylak D. Cytotoxic chemotherapy for advanced hormone-resistant prostate cancer. Cancer. 1993; 71(3 Suppl):1098–109. [PubMed: 7679039]

7. de Bono JS, et al. Prednisone plus cabazitaxel or mitoxantrone for metastatic castration-resistant prostate cancer progressing after docetaxel treatment: a randomised open-label trial. Lancet. 2010; 376(9747):1147–54. [PubMed: 20888992]

8. Tannock IF, et al. Docetaxel plus prednisone or mitoxantrone plus prednisone for advanced prostate cancer. N Engl J Med. 2004; 351(15):1502–12. [PubMed: 15470213]

9. Petrylak DP, et al. Docetaxel and estramustine compared with mitoxantrone and prednisone for advanced refractory prostate cancer. N Engl J Med. 2004; 351(15):1513–20. [PubMed: 15470214]

10. Jordan MA, Wilson L. Microtubules as a target for anticancer drugs. Nat Rev Cancer. 2004; 4(4): 253–65. [PubMed: 15057285]

11. Skipper HE. Kinetics of mammary tumor cell growth and implications for therapy. Cancer. 1971; 28(6):1479–99. [PubMed: 5127796]

12. Berges RR, et al. Implication of cell kinetic changes during the progression of human prostatic cancer. Clin Cancer Res. 1995; 1(5):473–80. [PubMed: 9816006]

13. Gascoigne KE, Taylor SS. Cancer cells display profound intra- and interline variation following prolonged exposure to antimitotic drugs. Cancer Cell. 2008; 14(2):111–22. [PubMed: 18656424]

14. Giannakakou P, et al. p53 is associated with cellular microtubules and is transported to the nucleus by dynein. Nat Cell Biol. 2000; 2(10):709–17. [PubMed: 11025661]

15. Mabjeesh NJ, et al. 2ME2 inhibits tumor growth and angiogenesis by disrupting microtubules and dysregulating HIF. Cancer Cell. 2003; 3(4):363–75. [PubMed: 12726862]

16. Carbonaro M, O'Brate A, Giannakakou P. Microtubule disruption targets HIF-1alpha mRNA to cytoplasmic P-bodies for translational repression. J Cell Biol. 192(1):83–99. [PubMed: 21220510]

17. Giannakakou P, et al. Enhanced microtubule-dependent trafficking and p53 nuclear accumulation by suppression of microtubule dynamics. Proc Natl Acad Sci U S A. 2002; 99(16):10855–60. [PubMed: 12145320]

18. Kuroda K, et al. Docetaxel down-regulates the expression of androgen receptor and prostate-specific antigen but not prostate-specific membrane antigen in prostate cancer cell lines: implications for PSA surrogacy. Prostate. 2009; 69(14):1579–85. [PubMed: 19575420]

19. Gan L, et al. Inhibition of the androgen receptor as a novel mechanism of taxol chemotherapy in prostate cancer. Cancer Res. 2009; 69(21):8386–94. [PubMed: 19826044]

20. Zhu ML, et al. Tubulin-targeting chemotherapy impairs androgen receptor activity in prostate cancer. Cancer Res. 2010; 70(20):7992–8002. [PubMed: 20807808]

21. Brass AL, et al. Androgen up-regulates epidermal growth factor receptor expression and binding affinity in PC3 cell lines expressing the human androgen receptor. Cancer Res. 1995; 55(14): 3197–203. [PubMed: 7606741]

22. Shen R, et al. Androgen-induced growth inhibition of androgen receptor expressing androgen-independent prostate cancer cells is mediated by increased levels of neutral endopeptidase. Endocrinology. 2000; 141(5):1699–704. [PubMed: 10803579]

23. Yuan S, et al. Androgen-induced inhibition of cell proliferation in an androgen-insensitive prostate cancer cell line (PC-3) transfected with a human androgen receptor complementary DNA. Cancer Res. 1993; 53(6):1304–11. [PubMed: 8443809]

24. Liu H, et al. Constitutive and antibody-induced internalization of prostate-specific membrane antigen. Cancer Res. 1998; 58(18):4055–60. [PubMed: 9751609]

25. Liu H, et al. Monoclonal antibodies to the extracellular domain of prostate-specific membrane antigen also react with tumor vascular endothelium. Cancer Res. 1997; 57(17):3629–34. [PubMed: 9288760]

26. Ding D, et al. Effect of a short CAG (glutamine) repeat on human androgen receptor function. Prostate. 2004; 58(1):23–32. [PubMed: 14673949]

27. Giannakakou P, et al. Paclitaxel-resistant human ovarian cancer cells have mutant beta-tubulins that exhibit impaired paclitaxel-driven polymerization. J Biol Chem. 1997; 272(27):17118–25. [PubMed: 9202030]

28. Burkhardt JK, et al. Overexpression of the dynamitin (p50) subunit of the dynactin complex disrupts dynein-dependent maintenance of membrane organelle distribution. J Cell Biol. 1997; 139(2):469–84. [PubMed: 9334349]

29. Riethdorf S, et al. Detection of circulating tumor cells in peripheral blood of patients with metastatic breast cancer: a validation study of the CellSearch system. Clin Cancer Res. 2007; 13(3):920–8. [PubMed: 17289886]

30. Schall R. Estimation in Generalized Linear-Models with Random Effects. Biometrika. 1991; 78(4):719–727.

31. Breslow NE, Clayton DG. Approximate Inference in Generalized Linear Mixed Models. Journal of the American Statistical Association. 1993; 88(421):9–25.

32. Wolfinger R, Oconnell M. Generalized Linear Mixed Models - a Pseudo-Likelihood Approach. Journal of Statistical Computation and Simulation. 1993; 48(3–4):233–243.

33. Scher HI, et al. Design and end points of clinical trials for patients with progressive prostate cancer and castrate levels of testosterone: recommendations of the Prostate Cancer Clinical Trials Working Group. J Clin Oncol. 2008; 26(7):1148–59. [PubMed: 18309951]

34. Ross JL, Ali MY, Warshaw DM. Cargo transport: molecular motors navigate a complex cytoskeleton. Curr Opin Cell Biol. 2008; 20(1):41–7. [PubMed: 18226515]

35. Perner S, et al. Prostate-specific membrane antigen expression as a predictor of prostate cancer progression. Hum Pathol. 2007; 38(5):696–701. [PubMed: 17320151]

36. Wang X, et al. Targeted treatment of prostate cancer. J Cell Biochem. 2007; 102(3):571–9. [PubMed: 17685433]

37. Armstrong AJ, et al. Prostate-specific antigen and pain surrogacy analysis in metastatic hormone-refractory prostate cancer. J Clin Oncol. 2007; 25(25):3965–70. [PubMed: 17761981]

38. Petrylak DP, et al. Evaluation of prostate-specific antigen declines for surrogacy in patients treated on SWOG 99–16. J Natl Cancer Inst. 2006; 98(8):516–21. [PubMed: 16622120]

39. Komlodi-Pasztor E, et al. Mitosis is not a key target of microtubule agents in patient tumors. Nat Rev Clin Oncol. 2011

40. Giannakakou P, et al. A common pharmacophore for epothilone and taxanes: molecular basis for drug resistance conferred by tubulin mutations in human cancer cells. Proc Natl Acad Sci U S A. 2000; 97(6):2904–9. [PubMed: 10688884]

41. Giannakakou, P.; Snyder, JP. Resistance to Microtubule-Targeting Drugs. In: Fojo, T., editor. The Role of Microtubules in Cell Biology, Neurobiology, and Oncology. Humana Press; 2008. p. 357-394.

42. Nettles JH, et al. The binding mode of epothilone A on alpha,beta-tubulin by electron crystallography. Science. 2004; 305(5685):866–9. [PubMed: 15297674]

43. Shaffer DR, et al. Circulating tumor cell analysis in patients with progressive castration-resistant prostate cancer. Clin Cancer Res. 2007; 13(7):2023–9. [PubMed: 17404082]

44. Attard G, et al. Characterization of ERG, AR and PTEN gene status in circulating tumor cells from patients with castration-resistant prostate cancer. Cancer Res. 2009; 69(7):2912–8. [PubMed: 19339269]

45. Stott SL, et al. Isolation and characterization of circulating tumor cells from patients with localized and metastatic prostate cancer. Sci Transl Med. 2(25):25ra23.

46. Grad JM, et al. Multiple androgen response elements and a Myc consensus site in the androgen receptor (AR) coding region are involved in androgen-mediated up-regulation of AR messenger RNA. Mol Endocrinol. 1999; 13(11):1896–911. [PubMed: 10551783]

47. Reid AH, et al. CYP17 inhibition as a hormonal strategy for prostate cancer. Nat Clin Pract Urol. 2008; 5(11):610–20. [PubMed: 18985049]

48. Tran C, et al. Development of a second-generation antiandrogen for treatment of advanced prostate cancer. Science. 2009; 324(5928):787–90. [PubMed: 19359544]
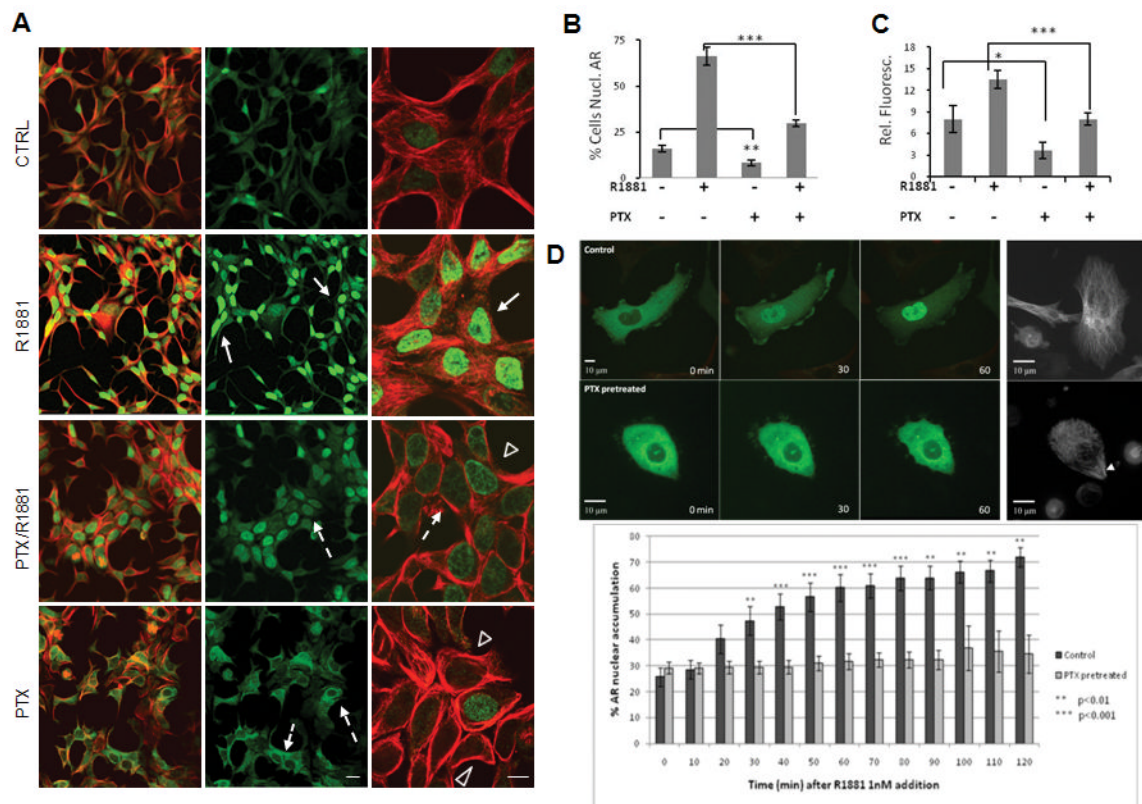
**Figure 1. Taxane treatment impairs AR nuclear accumulation**

(A) LNCaP cells were treated with DMSO (vehicle control) or paclitaxel (PTX) 100 nM overnight followed by 1 h treatment with the synthetic DHT analog R1881 (1 nM) to induce AR nuclear translocation. Cells were fixed and immunostained with antibodies against AR (green) and total tubulin (red) and imaged by confocal microscopy. Left panel: overlay of tubulin and AR, middle panel: AR alone, right panel: representative high magnification images of tubulin and AR. Solid arrows: AR nuclear localization in R1881 panel, Dashed arrow: AR cytoplasmic sequestration and reduced nuclear accumulation, Arrowheads: microtubule bundles. (B) Quantitative analysis of number of cells with AR nuclear staining. (C) Quantitation of relative AR nuclear fluorescence intensity. (D) Dynamics and quantitation of AR nuclear accumulation using live cell imaging of PC3:mCherry-Tub cells microinjected with GFP-AR and treated with 1nM R1881 in the absence or presence of 13M PTX. *Upper panel:* Time lapse images were obtained with a spinning disk confocal microscope by acquiring an entire Z-stack at 10 min intervals for 2 hr. Shown are maximum intensity projections of representative PC3:mCherry-Tub cells expressing full-length GFP-AR at the indicated time points (for the full 2 hr recording see movies S1 and S2). The integrity of the microtubule cytoskeleton from untreated of PTX treated cells was visualized with mCherry-tubulin at the end of the timelapse recording and is shown in the far right panels. Arrowhead points at microtubule bundles. *Lower Panel:* Graphic representation of AR nuclear accumulation over time following R1881 treatment in control versus PTX-pretreated cells. Quantitative analysis of nuclear of GFP-AR was performed on each focal plane (0.5 μm Z-sections through the entire cell depth) using integrated pixel intensity values from the sum projection and the percentage of nuclear AR was calculated using the following formula: % Nuclear AR = 100*Nuclear AR/Total AR. This analysis was performed on the following number of cells for each time point and treatment condition: Control 0–20 min: n=8; 30–110 min: n=7; 120 min: n=6. PTX pretreated 0–80 min: n=12;

90 min: n=8; 100–120 min n=3. Statistical analysis was performed using T-test with equal variances (** p<0.01; *** p<0.001).
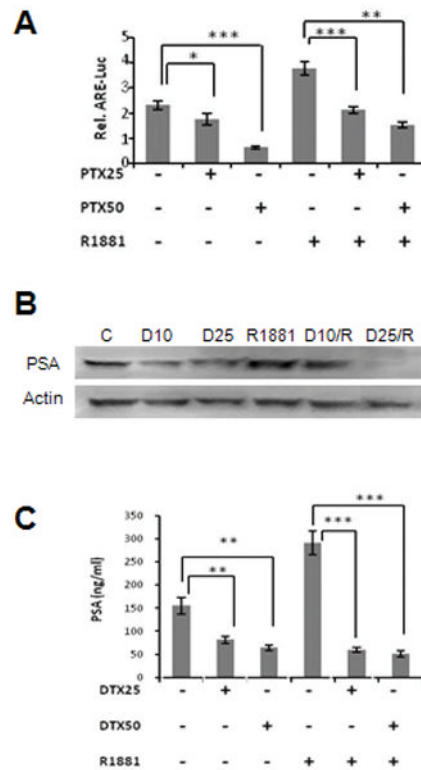
Figure 2. AR transcriptional activity is inhibited by taxane treatment
(A) LNCaP cells were transfected with ARE-luciferase reporter plasmid and treated overnight with the indicated concentrations of paclitaxel (PTX) in the presence or absence of R1881 (1 nM for 1 hr). AR transcriptional activity was measured using firefly luciferase values normalized to renilla luciferase to account for differences in transfection efficiency. (B) Endogenous PSA protein expression was assessed by immunoblotting of whole cell extracts from LNCaP cells treated overnight with the indicated concentrations of docetaxel (D) in the presence or absence of 1 hr treatment with 10 nM R1881 (R). Actin is shown as loading control. (C) Secreted PSA levels were measured (ng/mL) in conditioned media collected from LNCaP cells treated as is (F) with 25 or 50 nM of docetaxel (DTX). For all panels statistical values are * p<0.1; ** p<0.01; *** p<0.001)
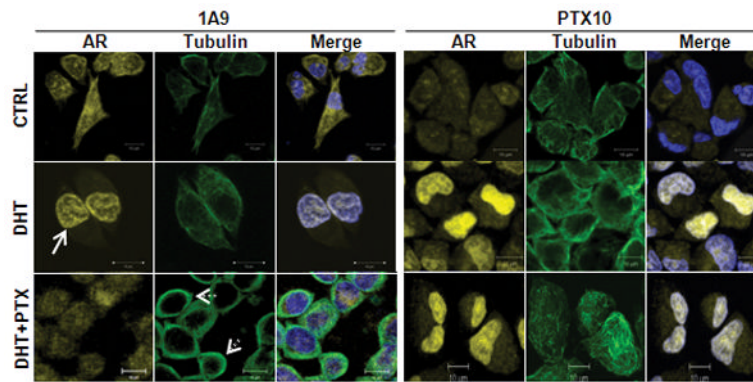
Figure 3. Taxane-induced AR cytoplasmic sequestration requires microtubule stabilization
Paclitaxel treatment has no effect on AR subcellular localization in β-tubulin mutant paclitaxel-resistant cells. Parental, 1A9, and paclitaxel-resistant 1A9/PTX10 ovarian cancer cells were stably transfected with GFP-AR, treated for 2hr with either DMSO or 100nM PTX followed by the addition of 100nM DHT for another 2hr. Cells were then fixed, stained for AR, tubulin and DAPI and imaged by point scanning confocal microscopy. Solid arrows: nuclear AR; dashed arrow: microtubule bundles
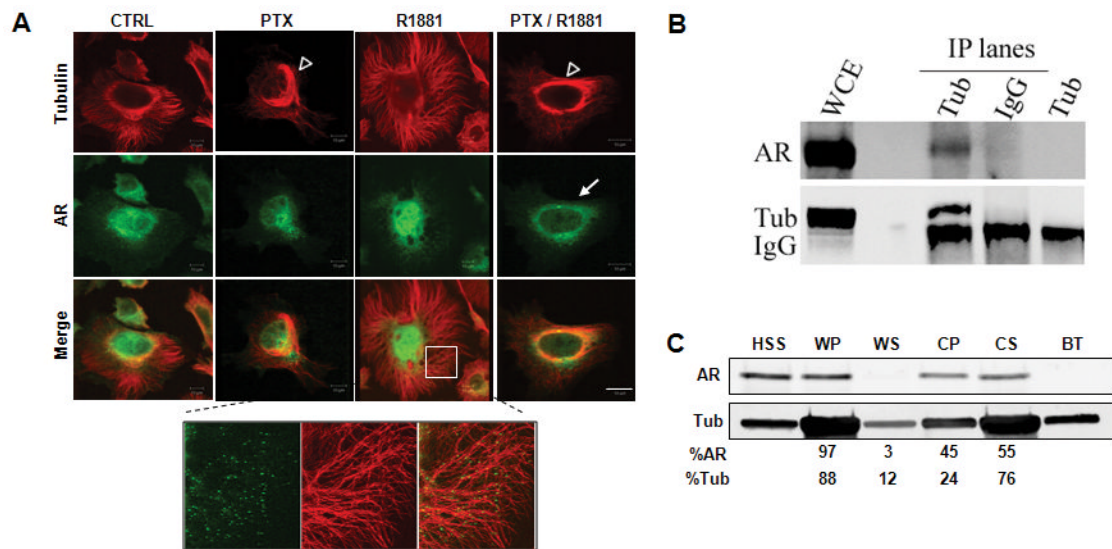
Figure 4. AR colocalizes and cofractionates with the microtubule cytoskeleton
AR colocalizes with microtubules. PC3-AR cells were treated and processed as in Fig. 1a.
Arrowhead: microtubule bundles, Solid Arrows: AR cytoplasmic sequestration at
perinuclear region. Note the co-localization with microtubule bundles. *Lower panel is a* high
magnification of the boxed cytoplasmic area depicting AR co-localization with the
microtubule network. (B) AR co-immunoprecipitates with tubulin. Whole cell extracts
(WCE) from LNCaP cells were immunoprecipitated with anti-tubulin antibody (Tub, lane 3)
and IgG control (IgG, lane 4) and immunoblotted for AR and tubulin. 50 μg of WCE (lane
1) and 2 μg of the tubulin antibody (Tub, lane 5) alone were loaded as controls. Lane 2 is
empty. (C) AR binds preferentially to the microtubule polymer. 50 μg of pre-cleared cell
extract (HSS) from LNCaP cells were incubated for 30min with exogenous purified bovine
brain tubulin that was either paclitaxel-stabilized at 37°C (WP and WS fractions) or
colchicine depolymerized on ice (CP and CS fractions). The samples were centrifuged at
100,000 g to separate the microtubule polymers (WP and CP) from the soluble tubulin
dimers (WS and CS), resolved by SDS-PAGE and immunoblotted for the presence of AR
and tubulin. The distribution of AR and tubulin in each respective fraction was calculated
based on the intensity of each band assessed by densitometry. For example, the percent
tubulin (%Tub) is calculated as the amount of polymerized tubulin (P) over the total amount
of polymerized and soluble tubulin (P + S) times 100 ($\%P = [P/(P + S)] \times 100$) based on
densitometric analysis. Similar analysis was performed for AR. Note that 97% of
endogenous AR co-fractionated with the majority of tubulin found in the WP microtubule
fraction, while upon partial tubulin depolymerization the AR-microtubule co-fractionation
decreased accordingly. HSS: high speed supernatant, WP: warm pellet, WS: warm
supernatant, CP: cold pellet, CS: cold supernatant, BT: bovine brain tubulin.
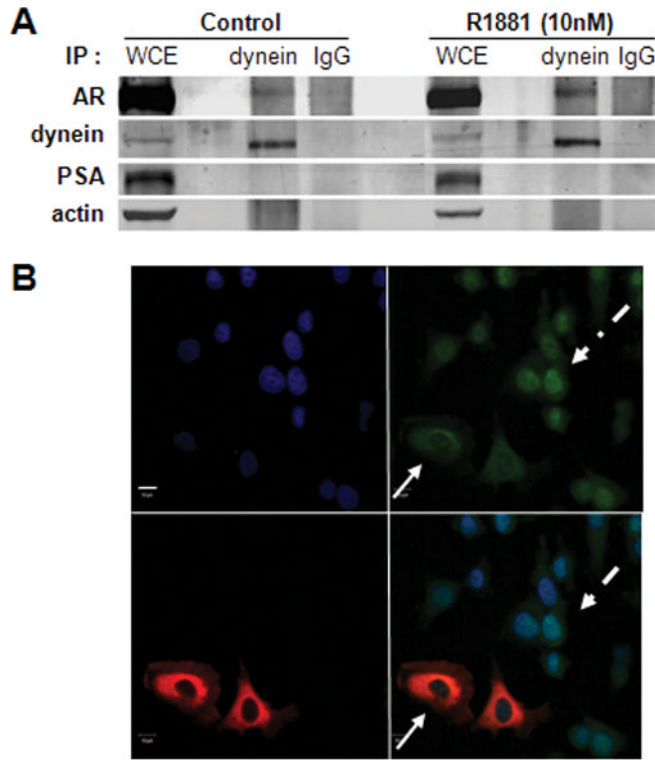
Figure 5. AR trafficking to the nucleus is mediated by the microtubule-motor protein dynein
(A) AR co-immunoprecipitates with the microtubule motor protein dynein. Total cell extract from wild type LNCaP cells (control or treated with 10nM R1881 for 1hr) was immunoprecipitated with a dynein antibody or control IgG and immunoblotted for the presence of AR, dynein, PSA and actin shown as negative controls. (B) Overexpression of dynamitin impairs ligand-stimulated AR nuclear accumulation. PC3-AR cells were transiently transfected with pCMVH50myc (encoding a c-myc tagged human dynamitin) and subjected to R1881 treatment for 1hr. Cells were fixed, processed for double immunofluorescence labeling with antiAR (green) and c-myc (red) antibodies and analyzed by confocal microscopy. Solid arrows point to cells overexpressing dynamitin. Dashed arrows point to neighboring non-transfected cells. Scale bar: 10 μm.
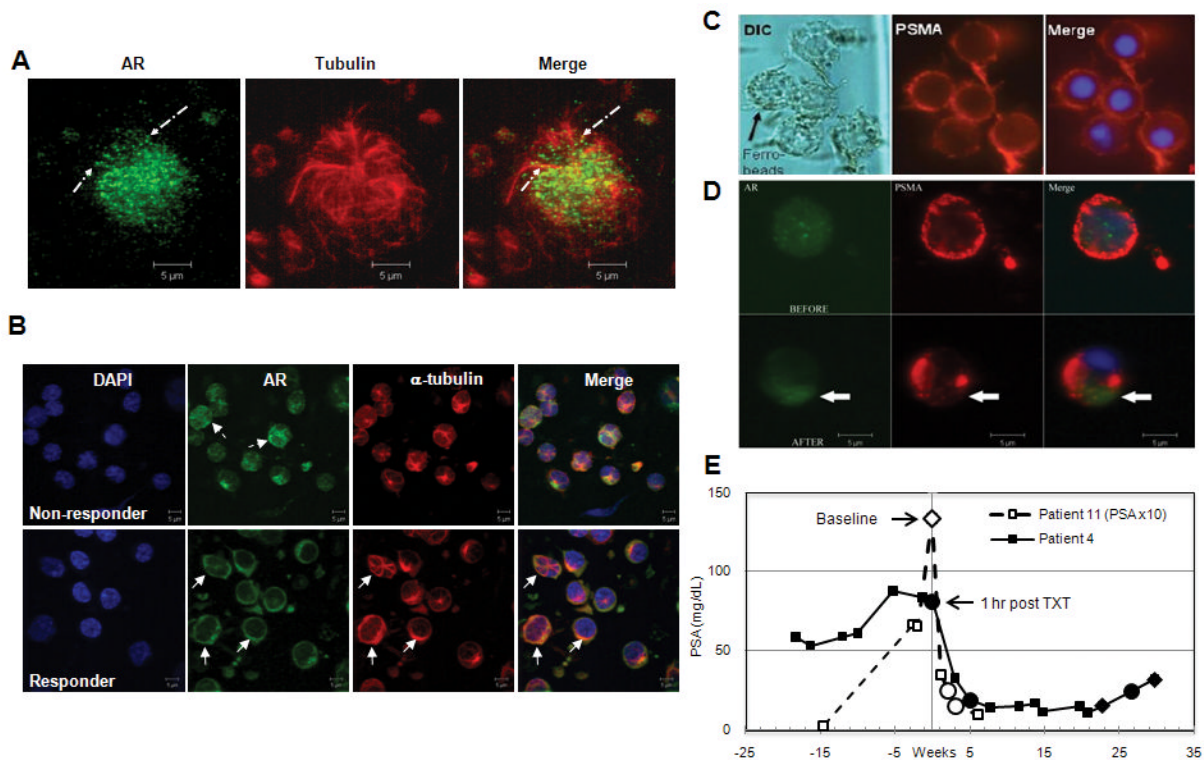
Figure 6. Clinical response to taxane-based chemotherapy correlates with AR cytoplasmic sequestration in CTCs

(A and B) PBMCs obtained from the blood of a metastatic CRPC patient following Ficoll separation were fixed and stained for DNA (DAPI), AR and tubulin. CTCs were defined as large (>10 μm diameter), nucleated, round to oval cells, expressing AR. (A) High magnification of a CTC showing that the cytoplasmic portion of AR colocalizes with MTs (dashed arrows). (B) Microtubule integrity and subcellular localization of AR in CTCs isolated from CRPC patients receiving chemotherapy. *Upper Panel:* CTCs identified from a metastatic docetaxel-resistant CRPC patient treated with paclitaxel (and carboplatin). CTCs analyzed 7 days following 2nd cycle of chemotherapy. Patient did not respond with rising PSA and increased sclerotic bone metastases on bone scan. Dashed arrows point to intense AR nuclear accumulation, indicative of active AR signaling. *Lower panel:* CTCs identified from previously untreated metastatic CRPC patient receiving docetaxel chemotherapy. CTCs analyzed 7 days post treatment following 10th cycle of chemotherapy. Patient responding to chemotherapy by PSA working group 2 criteria. The far right panel shows a merged image of all three fluorophores. Arrows point to bundled MTs and AR sequestration in the cytoplasm, suggesting inhibition of AR signaling. (C and D) CTCs were enriched from the blood of CRPC patient using EpCAM-coated ferrobeads, fixed and stained for DNA (DAPI), PSMA, AR and tubulin (not shown). (C) EpCAM-captured CTCs express the prostate specific membrane antigen (PSMA). Arrow in the DIC panel points at the ferrobeads used to specifically capture CTCs. The right panel depicts the merged image of PSMA and DAPI. (D) The AR localization in CTCs isolated from CRPC patient 11 is shifted from the nucleus at baseline to the cytoplasm (arrow), two weeks after receiving the first dose of chemotherapy. Note the complete lack of overlap between the AR and DAPI staining clearly indicating AR nuclear exclusion. (E) PSA trends over time for 2 representative CRPC patients receiving taxane based therapy. Blood was drawn and serum PSA was measured at the indicated time points. CTCs were isolated and stained for AR, tubulin and DAPI as in (D) to determine AR subcellular localization. Ovals and diamonds

on the graph represent the AR nuclear localization (cytoplasmic and nuclear, respectively) determined in CTCs isolated at these precise time points. For patient 11, evaluation of CTCs at baseline demonstrated the presence of AR in the nucleus. Following treatment, CTC analysis revealed a shift of AR to the cytoplasm, consistent with the decrease in PSA. CTCs from patient 4 demonstrated cytoplasmic AR during PSA response to taxane. However, CTCs subsequently showed AR nuclear localization before PSA progression was apparent.

Table 1

Comparison of AR Localization in Patient CTCs with PSA outcomes

Patient No. (Age)	Sample No.	Number of taxane cycle	AR localization	Total AR fluorescence intensity (RU)*	Clinical Response (PSAWG2)
1 (66)	1	5	Nuclear	149	Responder
2 (59)	1	4	Nuclear	177	Progressor
3 (62)	1	10	Cytoplasmic	69	Progressor
	1	1 hr post	Cytoplasmic	117	Baseline (1 hr post)
	2	2	Cytoplasmic	22	Responder
4 (70)	3	4	Nuclear	57	Progressor
	4	5	Cytoplasmic	66	Progressor
	5	6	Nuclear	82	Progressor
	6	6	Nuclear	274	Progressor
5 (78)	1	4	Nuclear	34	Progressor
	2	5	Nuclear	98	Progressor
6 (86)	1	4	Cytoplasmic	87	Responder
	2	5	Nuclear	71	Progressor
7 (69)	1	1	Cytoplasmic	NA	NA -- Stable
	2	4	Cytoplasmic	83	Progressor
	3	5	Nuclear	11	Progressor
8 (88)	1	6	Nuclear	114	Progressor
9 (77)	1	7	Nuclear	92	Progressor
	1	1	Nuclear	48	Progressor
10 (61)	2	4	Nuclear	65	Progressor
	3	6	Nuclear	353	NA -- Stable
	4	8	Nuclear	NA	Responder
11 (69)	1	Baseline	Nuclear	244	Baseline

Patient No. (Age)	Sample No.	Number of taxane cycle	AR localization	Total AR fluorescence intensity (RU)*	Clinical Response (PSAWG2)
	2	1	Cytoplasmic	31	Responder
	3	1	Cytoplasmic	105	Responder
	4	2	Cytoplasmic	72	Responder
	5	6	Cytoplasmic	203	Progressor
12 (88)	1	Baseline	Nuclear	90	Baseline
	2	1	Cytoplasmic	NA	NA – Stable
13 (86)	1	Baseline	Nuclear	134	Baseline
	2	1	Nuclear	153	Progressor
	3	3	Nuclear	NA	NA -- Stable
	4	3	Nuclear	NA	NA -- Stable
	5	4	Cytoplasmic	NA	NA -- Stable
	6	4	Cytoplasmic	NA	NA - Stable
	7	4	Cytoplasmic	798	Progressor
	1	baseline	nuclear	37	Baseline
	1	1 hr. post	nuclear	51	Baseline (1 hr post)
14 (68)	2	1	Cytoplasmic	NA	NA-Stable
	3	1	Cytoplasmic	NA	NA-Stable
	4	2	Cytoplasmic	NA	NA-Stable

AR subcellular localization and total fluorescence intensity were determined in CTCs isolated from the blood of 14 patients at different time points during the course of their taxane-based chemotherapy. Results were then correlated to the patients' P S A outcome at the time that the CTCs were evaluated. PSA clinical response (responder vs. progressor) was defined using established Prostate Cancer Working Group 2 (PSAWG2) criteria.

*
1 Relative Unit (RU) = 10,000 pixel intensity